High photostability in non-conventional coumarins with far-red/NIR emission through azetidinyl substitution

Albert Gandioso,[†,‖] Marta Palau,[†,‖] Roger Bresolí-Obach,[‡,‖] Alex Galindo,[†] Anna Rovira,[†] Manel Bosch,[§] Santi Nonell,[‡] Vicente Marchán*[,†]

[†]Secció de Química Orgànica, Departament de Química Inorgànica i Orgànica, IBUB, Universitat de Barcelona, Martí i Franquès 1-11, E-08028 Barcelona (Spain)
E-mail: vmarchan@ub.edu
[‡]Institut Químic de Sarrià, Universitat Ramon Llull, E-08017 Barcelona (Spain)
[§]Unitat de Microscòpia Òptica Avançada, Centres Científics i Tecnològics, Universitat de Barcelona, E-08028 Barcelona (Spain)

[‖]These authors contributed equally to this work.

TOC ABSTRACT GRAPHIC

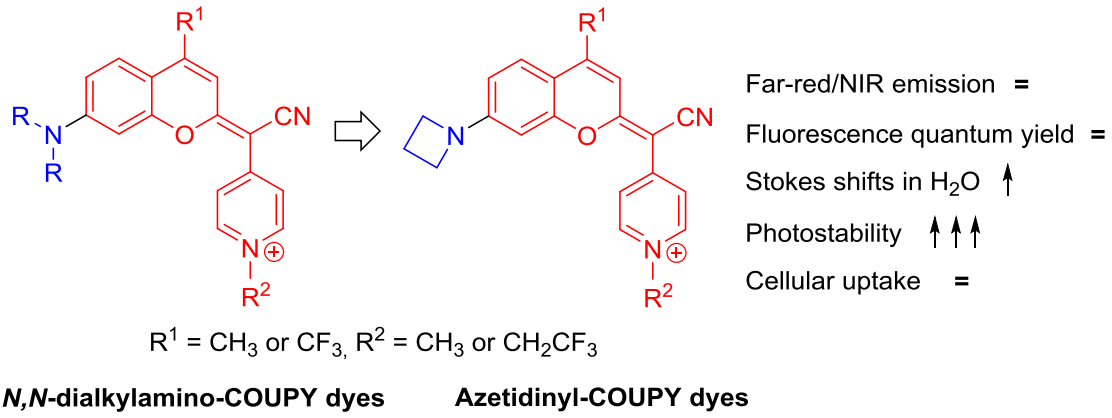

ABSTRACT

Replacement of electron-donating *N*,*N*-dialkyl groups with three or four-membered cyclic amines (e.g., aziridine and azetidine, respectively) has been described as a promising approach to improve some of the drawbacks of conventional fluorophores, including low fluorescent quantum yields (Φ_F) in polar solvents. In this work we have explored the influence of azetidinyl substitution on non-conventional coumarin-based COUPY dyes. Two azetidine-containing scaffolds were first synthesized in four linear synthetic steps and easily transformed into far-red/NIR-emitting fluorophores through *N*-alkylation of the pyridine moiety. Azetidine introduction in COUPY dyes resulted in enlarged Stokes' shifts with respect the *N*,*N*-dialkylamino-containing parent dyes, but the Φ_F were not significantly modified in aqueous media, which is in contrast with previously reported observations in other fluorophores. However, azetidinyl substitution led to an unprecedented improvement in the photostability of COUPY dyes and high cell permeability was retained since the fluorophores accumulated selectively in mitochondria and nucleoli of HeLa cells. Overall, our results provide valuable insights for the design and optimization of novel fluorophores operating in the far-red/NIR region, since we have demonstrated that three important parameters (Stokes' shifts, Φ_F and photostability) cannot be always simultaneously addressed by simply replacing a *N*,*N*-dialkylamino group with azetidine, at least in non-conventional coumarin-based fluorophores.

INTRODUCTION

In recent years we are witnessing a new resurgence in the use of fluorophores based on small organic molecules on advanced biological imaging techniques.[1] Current research efforts are focused on (i) the development of novel far-red and near-infrared (NIR) fluorophores by using modern chemical synthetic tools, (ii) fine-tuning their photophysical properties (e.g., absorption and emission wavelengths, fluorescence quantum yields and lifetimes, Stokes shifts and photostability) and (iii) improving their physicochemical properties (e.g., aqueous solubility and cell permeability), which are all together required for the applications of fluorescence microscopy in biological systems.[2] Although numerous fluorophores are currently available, *in vivo* applications such as fluorescence-guided surgery urgently demand novel efficient, cell-permeable fluorescent probes based on low molecular-weight scaffolds operating in the optical window of the tissues.[3]

Since the discovery of umbelliferone (7-hydroxycoumarin) at the end of the nineteenth century,[1d] coumarins have been traditionally used as fluorescent organic molecules owing to their well-stablished photophysical properties and good cell permeability, and nowadays some coumarin derivatives (e.g., Alexa Fluor 350) are still being used in fluorescence microscopy. However, the fact that conventional coumarins such as Coumarin 1 (compound **1** in Scheme 1) require UV excitation hampers most *in vivo* applications due to the toxicity of this radiation and its low capacity of penetration in biological tissues. For this reason, great efforts have been dedicated in the last decades to red-shift absorption and emission of coumarins into the blue-green-red region of the visible spectrum by introducing electron-withdrawing groups (EWG) at the coumarin skeleton, by extending the π–conjugation system through position 3,[4] or by fusion of aromatic cycles,[5] including other fluorescent scaffolds.[6]

Although the majority of the abovementioned coumarin derivatives maintain the electron-withdrawing lactone moiety of the original umbelliferone, which creates a push-pull effect with electron-donating groups incorporated at position 7 (e.g., *N*,*N*-dialkylamino or hydroxy/alkoxy), in recent years some groups have demonstrated that absorption and emission of these chromophores can also be red-shifted by modifying it. Indeed, green light emission was accomplished either through thionation of the carbonyl group or by extending the conjugation of the system at position 2 with a dicyanomethylene group, being the applications of dicyanomethylene-caged oligonucleotides and cyclic RGD-containing particularly appealing.[7] Very recently, we have reported the synthesis of novel coumarins in which one cyano group of dicyanocoumarin derivatives was replaced by a phenyl ring containing EWGs[8] or by the electron-deficient pyridine heterocycle[9] with the aim of further

increasing the push-pull character of the coumarin chromophore. The later coumarin scaffolds (compounds **2** and **3** in Scheme 1) allowed us to develop a new family fluorophores, nicknamed COUPY, whose photophysical properties can be easily tuned by selecting the appropriate combination of the *N*-alkylating group at the pyridine moiety and the substituent at position 4 of the coumarin skeleton (compounds **4-7** in Scheme 1).[9] Taking into account their low molecular weight, COUPY dyes offer many attractive features such as large Stokes' shifts, brightness and emission in the far-red/NIR region, as well as aqueous solubility and good cell permeability. Such novel fluorophores opened the way to solving some of the main drawbacks associated with conventional coumarin-based fluorophores.

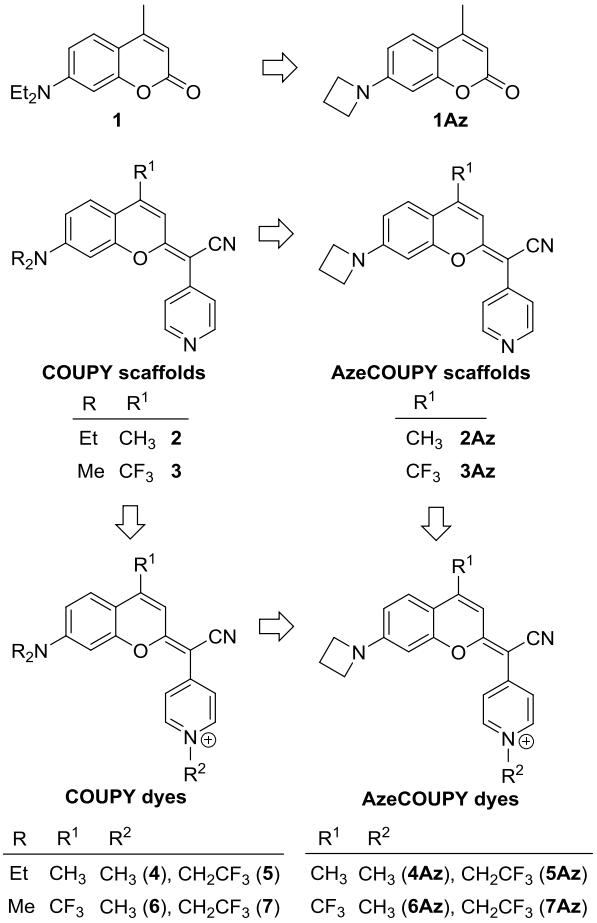

Scheme 1. Rational design of 7-azetidinyl-containing coumarin fluorophores.

Recently, Lavis and collaborators described that replacement in conventional fluorophores of electron-donating *N*,*N*-dialkyl groups (e.g., rhodamines, coumarins, naphthalimides, acridines, etc.) with azetidine allows to increase the fluorescent quantum yield (Φ_F) in polar solvents.[10] A similar behavior was described by Liu, Xu and co-workers when the three-membered aziridine ring was used.[11] These structural modifications, as well as other based on

cyclic amines,[12] have been postulated to suppress twisted intramolecular charge transfer formation (TICT), which is one of the major non-radiative de-excitation pathways in many fluorophores containing *N,N*-dialkyl motifs. Indeed, twisting of the *N,N*-dialkylamino group out the fluorophore plane upon photoexcitation forms a non-emissive and short-lived reactive chemical species, which can be avoided through structural modifications and rigidification. Rivera-Fuentes and co-workers have demonstrated that azetidinyl substituent can also be exploited to modulate photochemical processes in coumarin-based caging groups.[13] In addition, they have proposed a mechanism of fluorescence quenching for coumarin **1** that does not involve TICT states but rather H-bond induced non-radiative decay (HBIND).[14] Such unproductive decay channel was inhibited in **1Az** analogue (Scheme 1) by azetidinyl substitution.

Taking into account all the antecedents on azetidinyl-substituted fluorophores, we set out to study how this modification could influence the photophysical and physicochemical properties of coumarin-based COUPY dyes (**4-7**, Scheme 1). With this idea in mind, herein we describe the synthesis and photophysical characterization of azetidinyl analogues of COUPY fluorophores (**4Az-7Az**, Scheme 1), in which diethyl- or dimethylamino groups at position 7 of the coumarin skeleton have been replaced by the four-membered azetidine ring. Surprisingly, the fluorescent quantum yield of the resulting 7-azetidinyl-COUPY fluorophores was not significantly modified in aqueous media with respect their dialkylamino analogues. However, azetidinyl substitution led to a substantial improvement in photostability and larger Stokes' shifts in polar solvents relative to the parent *N,N*-dialkylamino COUPY dyes, while emission was kept in the optimal far-red/NIR region. High cell permeability was retained after azetidine incorporation and the fluorophores accumulated selectively in mitochondria and nucleoli of HeLa cells as occurred with their parent *N,N*-dialkylamino dyes. Overall, our results provide valuable insights for the design and optimization of fluorophores operating in the far-red/NIR region.

RESULTS AND DISCUSSION

Design, synthesis and characterization of 7-azetidinyl-coumarin fluorophores

The synthesis of azetidinyl-coumarin scaffolds **2Az** and **3Az** was first explored by following an straightforward methodology recently developed by us for the preparation of the parent *N*,*N*-dialkylamino-COUPY scaffolds **2** and **3**,[9] which makes use of thiocoumarin precursors (Scheme 2). Unfortunately, the reaction of azetidinyl-coumarin **1Az**[10] with Lawesson's reagent (LW) did not afford the expected compound (**8**) but several side-products, most of them resulting from the reaction of the thionating reagent with the azetidine moiety, as inferred by HPLC ESI-MS analysis (Scheme 2). Azetidine ring-opening occurred even under milder conditions (e.g., 60 ºC).

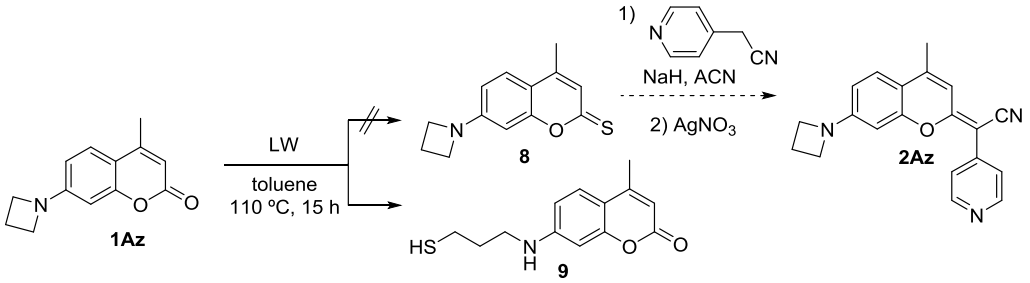

Scheme 2. Reaction of 7-azetidinyl-coumarin **1Az** with Lawesson's reagent.

Taking into account the high reactivity of azetidine with Lawesson's reagent, an alternative synthetic route for the preparation of **2Az** and **3Az** was explored (Scheme 3) in which thionation and the formation of the exocyclic C=C double bond would occur before the incorporation of the four-membered azetidine heterocycle. Starting from commercially available 7-hydroxycoumarins (**10a** and **10b**), reaction with trifluoromethanesulfonic anhydride in pyridine conduced to the expected triflate derivatives (**11a** and **11b**, respectively) in near quantitative yield.[15] In this case, thionation with LW under standard conditions (reflux in toluene, overnight) afforded the expected 7-triflylthiocoumarins (**12ab**). The next step involved condensation of **12a** and **12b** with 4-pyridylacetonitrile to provide coumarins **13a** (44%) and **13b** (57%), respectively, after silica column chromatography. Finally, the azetininyl function at position 7 was introduced through Buchwald-Hartwig amination.[16] The carbon-nitrogen bond was formed via the palladium-catalyzed cross-coupling of azetidine with 7-triflylcoumarins (**13ab**) by using RuPhos-Pd-G3 and RuPhos as pre-catalyst and ligand, respectively, and potassium carbonate as base. After a two-step purification process (silica column chromatography followed by filtration through a HLB

cartridge), the two pure azetidinyl-COUPY scaffolds (**2Az** and **3Az**) were isolated (60% and 48% yield, respectively) and fully characterized by HR ESI-MS and ^{1}H and ^{13}C NMR.

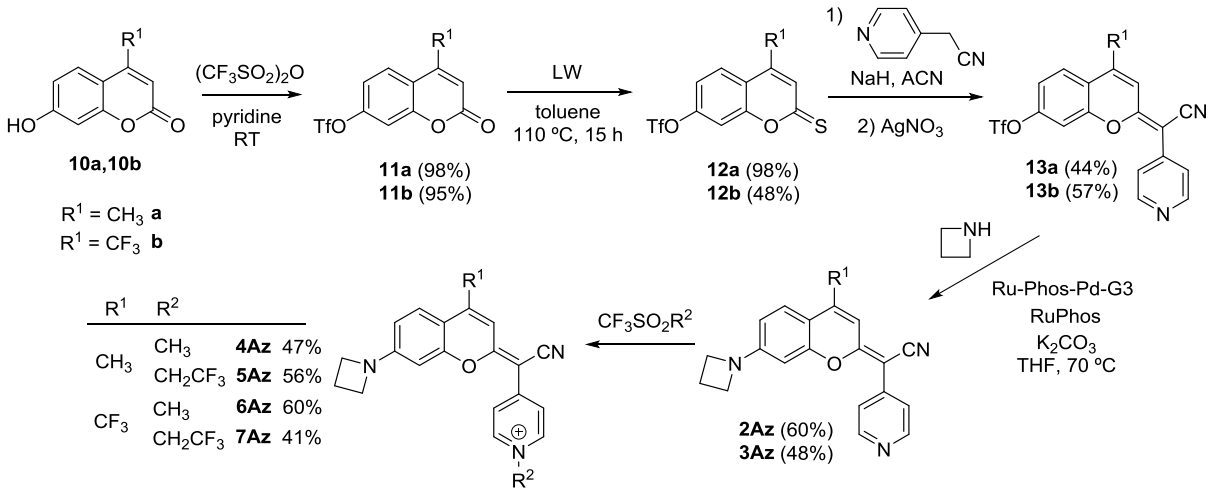

Scheme 3. Synthesis of 7-azetidinyl-COUPY scaffolds (**2Az** and **3Az**) and their corresponding *N*-alkylated fluorophores (**4Az-7Az**).

As previously found with the parent COUPY scaffold **2** (Scheme 1),[9] the ^{1}H NMR spectrum of **2Az** showed two sets of proton signals in an ~93:7 ratio (Figure 1). $^{1}H–^{1}H$ NOESY experiments (Figures 1 and S1) confirmed the existence of *E* and *Z* interconverting rotamers in solution around the exocyclic carbon-carbon bond and that the *E* rotamer was the one preferred. In the case of the 4-CF_3 analogue (**3Az**), the *E* rotamer was the major species identified (Figure S2).

Having at hand the two azetidinyl-COUPY scaffolds, we synthesized the corresponding *N*-alkylated pyridinium derivatives following our previously described methodology.[9] As shown in Scheme 3, reaction of **2Az** and **3Az** with methyl trifluoromethanesulfonate afforded *N*-methylpyridinium-coumarin dyes **4Az** and **6Az**, respectively. Similarly, the use of 2,2,2-trifluoroethyl trifluoromethanesulfonate allowed to obtain azetidinyl-COUPY dyes **5Az** and **7Az**. The four new coumarin derivatives were isolated after silica column chromatography as purple (**4Az-6Az**) and dark blue (**7Az**) solids, and their purity was assessed by HPLC (Figure S3). Characterization was carried out HR ESI-MS and 1D (^{1}H, ^{13}C, and ^{19}F) and 2D NMR. Similarly to parent COUPY dyes, the *E* rotamer was the major species for the corresponding 7-azetidinyl derivatives **4Az**, **5Az** and **7Az**, while around 7% of rotamer Z was identified for **6Az** (Figures S4−S7).

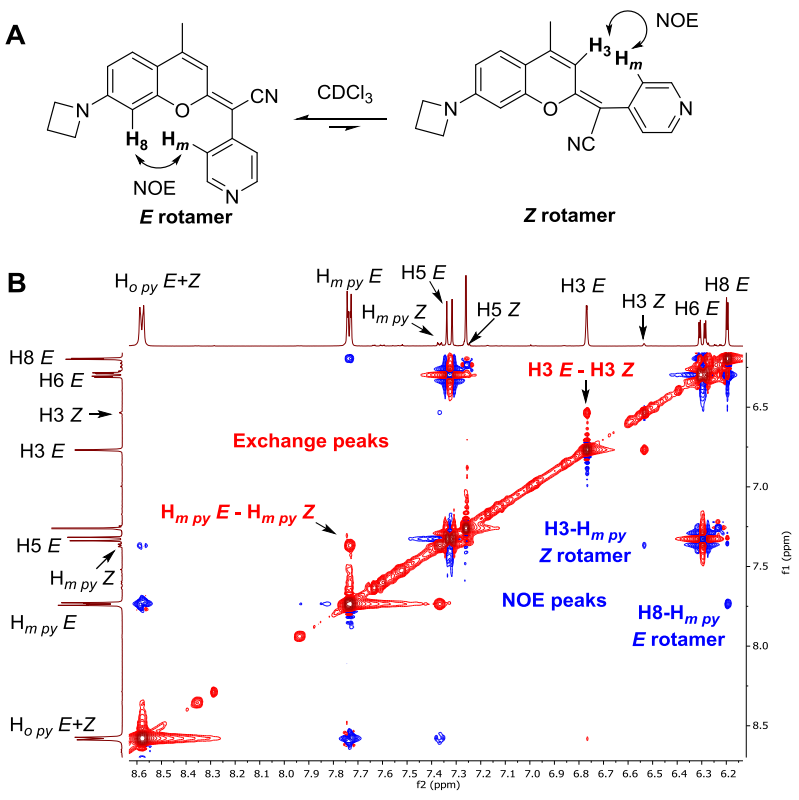

Figure 1. (A) Structures of the *E* and *Z* rotamers of coumarin **2Az** with some diagnostic NOE cross-peaks indicated. (B) Expansion of the 2D NOESY spectrum (t_m = 500 ms, 25 °C) of **2Az** in $CDCl_3$ showing exchange cross-peaks between rotamer resonances of the same sign as the diagonal.

Photophysical characterization of 7-azetidinyl-COUPY fluorophores.

The spectroscopic and photophysical properties of 7-azetidinyl-COUPY fluorophores (**4Az-7Az**) were investigated to assess the effect of replacing the 7-*N*,*N*-dialkylamino group in COUPY dyes by the four-membered azetidine ring. The UV-Vis absorption and emission spectra of the compounds were collected in six solvents of different polarity and viscosity (see Figure 1 and Figures S8-S11). The photophysical properties of **4Az-7Az** are summarized in Tables 1, S1 and S2 and compared with those of their parent 7-*N*,*N*-dialkylamino-COUPY dyes (**4-7**, respectively).[9] As shown in Figure 2, the new 7-azetidinylcoumarins reproduced the trend previously found with **4-7** and provided intense coloured solutions due to the existence of an intense absorption band in the visible spectrum, with absorption maxima ranging from 515 nm (**4Az**) to 592 nm (**7Az**) in aqueous solution (PBS buffer), and from 566 nm (**4Az**) to 630 nm (**7Az**) in DCM. Such bathochromic effects with respect conventional coumarins (e.g., compare with 7-azetidinylcoumarin **1Az**: λ_{abs} = 355 nm in H_2O)[13] are a consequence of the lengthening of the conjugated chromophore and the increased push−pull character of the conjugated system in COUPY dyes. The absorption maximum of 4-CF_3

derivatives (**6Az** and **7Az**) was significantly red-shifted with respect the 4-CH_3 coumarins (**4Az** and **5Az**) (from 25 to 47 nm, depending on the compounds and on the solvent). Moreover, the incorporation of a second strong electron-withdrawing CF_3 group moiety led to an additional red-shift in the absorption maximum (e.g., compare λ_{abs} = 541 and 607 nm for **6Az** and λ_{abs} = 592 and 630 nm for **7Az** in PBS and DCM, respectively).

As previously found with the parent *N*,*N*-dialkylamino dyes **4-7**, the 7-azetidinyl-COUPY analogues showed negative solvatochromism since an increase in the solvent polarity led to a significant blue-shift in their absorption maxima (e.g., for **4Az**, λ_{abs} = 515 nm in PBS and 566 nm in DCM). However, this effect was much pronounced in azetidinyl-containing dyes than in their corresponding parent compounds (e.g., compare data for **4Az** with that for **4**: λ_{abs} = 545 nm in PBS and 569 nm in DCM), which suggests that replacement of the dialkylamino group by azetidine is accompanied by an increase of the difference between ground and excited state dipole moments (Figure S10 and Table S2). This blue-shift in absorption maxima in H_2O upon azetidinyl substitution was also previously found for conventional coumarin **1** (e.g., compare λ_{abs} = 381 nm for **1** *vs* λ_{abs} = 355 nm for **1Az)**.[13] By contrast, the molar absorption coefficients (ε) of 7-azetidinyl-COUPY dyes were not significantly influenced by the polarity of the solvent, which is the opposite trend that we previously found for 7-*N*,*N*-dialkylamino-COUPY dyes in which a slight hyperchromism was showed in less-polar solvents. In general, the azetidine-containing COUPY dyes exhibited ε values smaller than those of the parent 7-*N*,*N*-dialkylamino dyes.

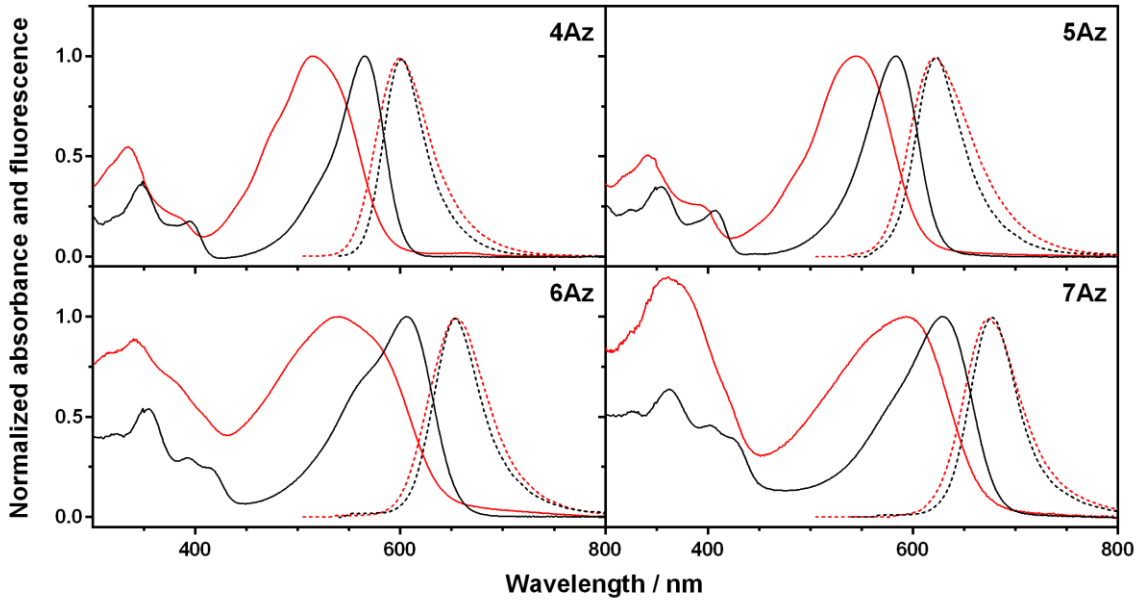

Figure 2. Comparison of the normalized absorption (solid lines) and fluorescence (dotted lines) spectra of 7-azetidinyl-COUPY dyes (compounds **4Az-7Az**) in toluene (black lines) and in PBS buffer (red lines).

7-Azetidinyl derivatives (**4Az-7Az**) reproduced the behavior of 7-*N*,*N*-dialkylamino-COUPY dyes (**4-7**) and showed emission in the far-red to NIR region (Figures 1 and S9), with the emission maximum ranging from 605 nm (**4Az**, ACN) to 681 nm (**7Az**, ACN). As shown in Tables 1 and S1, the compounds' emission maxima showed a slight blue-shift with respect the *N*,*N*-dialkylamino series in polar solvents (*ca* 4-8 nm; e.g., λ_{em} = 675 nm for **7Az** and λ_{em} = 682 nm for **7** in PBS), which parallels the solvent effect on the compounds' absorption maxima. As a result, 7-azetidinyl-COUPY dyes (except **7Az**) exhibited larger Stokes' shifts in polar solvents compared with their 7-*N*,*N*-dialkylamino parent dyes (e.g., 112 nm for **6Az** *vs* 92 nm for **6** in PBS buffer). Such large Stokes' shifts could find application in Förster-type resonance energy-transfer (FRET) experiments where a good separation between excitation and emission bands result in better contrast. As previously found with the parent 7-*N*,*N*-dialkylamino-COUPY dyes, the absorption and emission maxima for the 7-azetidinyl derivatives (**4Az-7Az**) was not significantly modified by changing the pH (Figure S11).

Table 1. Photophysical properties of 7-azetidinyl-COUPY dyes **4Az-7Az** in different solvents. The data for coumarin derivatives **4-7** has been included for comparison purposes.[9]

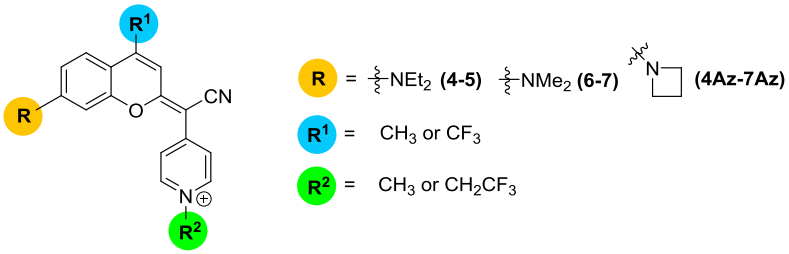

R^1, R^2	Solvent	λ_{abs} (nm)		ε ($mM^{-1}cm^{-1}$)		λ_{em} (nm)		Stokes'shift (nm)		Φ_F		τ_F (ns)	
		4	**4Az**	**4**	**4Az**	**4**	**4Az**	**4**	**4Az**	**4**	**4Az**	**4**	**4Az**
R^1=CH_3 R^2=CH_3	PBS	545	515	34	20	604	599	59	84	0.12	0.11	0.9	0.8
	ACN	548	541	75	23	609	605	61	64	0.18	0.21	1.4	1.4
	Toluene	566	563	47	23	601	604	35	41	0.64	0.82	4.8	4.7
		5	**5Az**	**5**	**5Az**	**5**	**5Az**	**5**	**5Az**	**5**	**5Az**	**5**	**5Az**
R^1=CH_3 R^2=CH_2CF_3	PBS	562	545	39	24	630	622	68	77	0.02	0.03	0.3	0.4
	ACN	567	561	43	24	636	627	69	66	0.12	0.03	1.2	0.7
	Toluene	582	580	47	22	625	625	43	45	0.54	0.64	5.4	4.9
		6	**6Az**	**6**	**6Az**	**6**	**6Az**	**6**	**6Az**	**6**	**6Az**	**6**	**6Az**
R^1=CF_3 R^2=CH_3	PBS	568	541	14	21	660	653	92	112	0.022	0.025	0.2	0.4
	ACN	569	567	47	20	668	661	99	94	0.023	0.02	0.2	0.4
	Toluene	601	607	20	20	657	658	56	51	0.19	0.24	2.4	3.1
		7	**7Az**	**7**	**7Az**	**7**	**7Az**	**7**	**7Az**	**7**	**7Az**	**7**	**7Az**
R^1=CF_3 R^2=CH_2CF_3	PBS	595	592	8.3	9.5	682	675	87	83	0.043	0.024	0.5	0.6
	ACN	597	602	26	16	689	681	92	79	0.12	0.063	1.4	1.7
	Toluene	619	625	18	11	683	680	64	55	0.20	0.15	3.3	3.2

As shown in Tables 1 and S1, 4-CH_3 azetidinyl dyes (**4Az** and **5Az**) exhibited excellent Φ_F in less-polar solvents (e.g., 0.82 and 0.64 in toluene, respectively) whereas the fluorescence quantum yields for the 4-CF_3 analogues (**6Az** and **7Az**) were moderate (e.g., 0.24 and 0.15 in toluene, respectively). To our surprise fluorescence quantum yields (Φ_F) of all the azetidinyl dyes both in polar protic and nonprotic polar solvents were similar (e.g 0.21 for **4Az** and 0.18 for **4** in ACN) or even slightly lower than those of the parent *N*,*N*-dialkylamino-containing dyes (e.g., 0.06 for **7Az** and 0.12 for **7** in ACN). As previously stated, the stabilization of the TICT excited state is a major cause for fluorescence quenching in polar solvents for many conventional fluorophores, although HBIND has been recently postulated as a deactivation mechanism of the excited state of coumarin **1**.[13] Replacement of the 7-*N*,*N*-dialkylamino group in conventional coumarins with azetidine lead to a clear improvement in the fluorescent quantum yield of the fluorophore. (e.g., Φ_F = 0.06 for **1** and Φ_F = 0.92 for **1Az** in H_2O).[13]

Interestingly, Φ_F values in glycerol (Table S1) were slightly lower in the azetidinyl-COUPY dyes (except for **4Az**, which was higher) compared with *N*,*N*-dialkylamino-containing parent dyes, and similar fluorescence lifetime (τ_F) values were obtained in this viscous polar solvent by time-resolved fluorescence spectroscopy (Figure S12). Overall, all these observations indicate that fluorescence quenching of non-conventional coumarin-based COUPY fluorophores in polar media cannot be exclusively attributed to the formation of a TICT excited state or to HBIND, which should had been prevented in their 7-azetidinyl-COUPY analogues, but to other competing deactivation channels.

Very importantly, the photostability of azetidinyl-COUPY dyes was considerably increased in aqueous media relative to the *N*,*N*-dialkylaminocounterparts. As shown in Figure 3, the photostability of coumarin **4Az** was similar to that of **4**, while **5Az** was photostable up to light fluences 3.3-fold higher than in the case of **5**. The large photostability of the 4-CF_3 series is particularly appealing since these compounds are photostable up to light fluences larger than 200 (**7Az**) and 400 (**6Az**) J/cm^2, fluences that are more than 10- and 20-fold, respectively, higher than those used for cellular imaging experiments.[17]

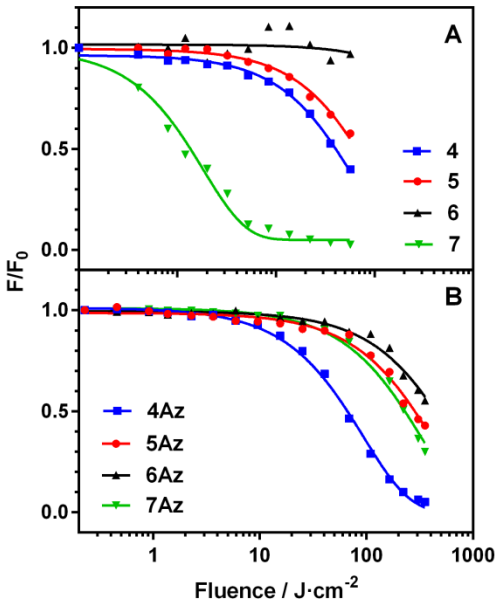

Figure 3. Fluorescence bleaching of COUPY (**4-7**) (A) and azetidinyl-COUPY dyes (**4Az-7Az**) in PBS buffer (5 μM) irradiated with green light (524 ± 17 nm; 8 mW/cm^2). Fluorophores: **4,4Az** (blue squares), **5,5Az** (red circles), **6,6Az** (black diamonds) and **7,7Az** (green triangles).

Table 2. Values of fluence (J/cm^2) where the fluorescence of COUPY (**4-7**) and azetidinyl-COUPY dyes (**4Az-7Az**) is reduced to the half.

	COUPY dyes	**Azetidinyl-COUPY dyes**
4-4Az	57	65
5-5Az	89	289
6-6Az	--	442
7-7Az	1.8	226

In summary, the replacement of *N*,*N*-dialkylamino groups with azetidine in conventional coumarins (e.g., **1** *vs* **1Az**) and in non-conventional coumarins such as COUPY dyes (e.g., **4-7** *vs* **4Az-7Az**) leads to significant differences in their photophysics (Figure 4). The larger blue-shifts in the absorption spectra of **4Az-7Az** in polar solvents indicate that their ground state is more polar than the excited state when compared with **4-7**. However, azetidinyl substitution does not significantly modify the position of the emission wavelength. As a result, azetidinyl-COUPY dyes show enlarged Stokes shifts in polar solvents compared with their parent COUPY dyes.

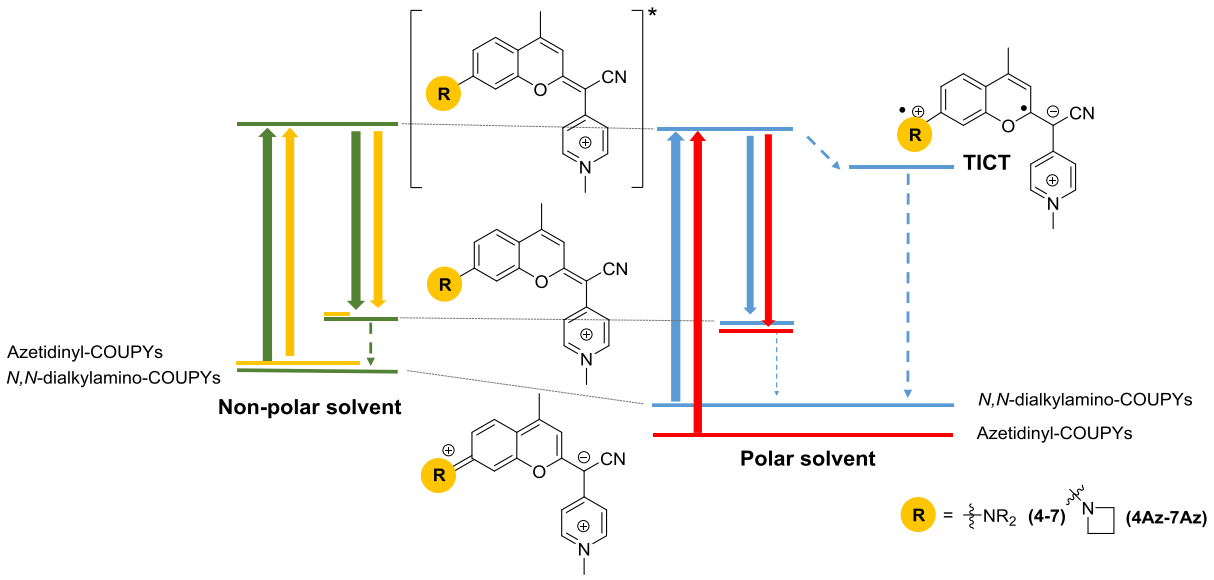

Figure 4. Comparison of the effect of replacing *N*,*N*-dialkylamino groups with azetidine in the solvatochromic properties of COUPY dyes, as exemplified with compounds **4** and **4Az**.

Fluorescence imaging of 7-azetidinyl-COUPY dyes in living cells

Having stablished how azetidine substitution influences the photophysical properties of the azetidinyl derivatives of COUPY dyes, we investigated their cellular uptake in living cells by using confocal microscopy. Compounds **4Az** to **6Az** were irradiated with a yellow light laser (λ_{ex} = 561 nm) and **7Az** with a red one (λ_{ex} = 633 nm). As shown in Figure 5, fluorescence was clearly observed in all cases in different cellular organelles after 30 min of incubation with the compounds, thereby confirming a good uptake by HeLa cells. Moreover, azetidinyl-COUPY dyes reproduced the same pattern of staining than their *N*,*N*-dialkylamino parent fluorophores (**4-7**) since mitochondria and nucleoli were clearly stained, together with intracellular vesicles.[9] This subcellular localization of **4Az** was confirmed with co-localization experiments using commercially available specific markers for labelling mitochondria (MitoTracker Green FM, MTG), lysosomes (Lysotracker Green FM, LTG) and nuclei (Hoechst 33342). In addition, accumulation into nucleoli was further investigated through enzymatic digestion with RNase A.

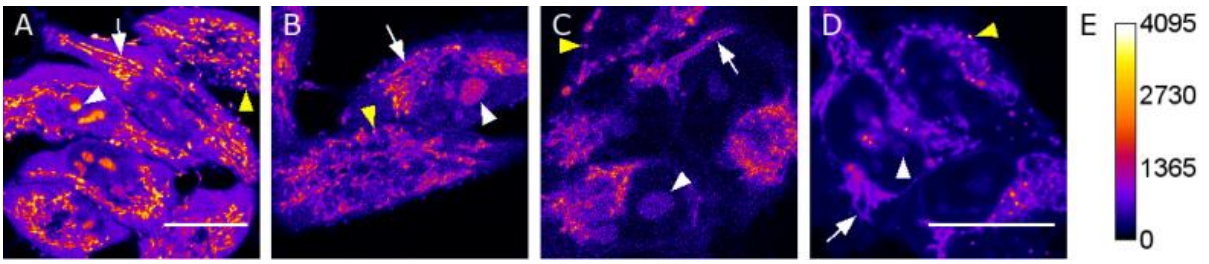

Figure 5. Cellular uptake of azetidinyl-COUPY dyes **4Az** (A), **5Az** (B), **6Az** (C) and **7Az** (D). Single confocal planes of HeLa cells incubated with the compounds (5 μM) during 30 min at 37ºC. Coumarins **4Az** to **6Az** were excited at 561 nm and emission detected from 570 to 670 nm, and **7Az** was excited at 633 nm and emission detected from 650 to 750 nm. White arrows point out mitochondria, white arrowheads nucleoli and yellow arrowheads vesicles staining. All images are colour coded using the Fire lookup table from Fiji (intensity calibration bar is showed in E). Scale bar: 10 μm. B C are at the same scale than A.

As shown in Figures 6 and S13, the accumulation of COUPY dyes into the mitochondria was confirmed by comparing the distribution of the fluorescence emission of **4Az** with that of Mitotracker Green. Co-localization was measured using two different coefficients, the Pearson's and Manders' (M1 and M2) coefficients,[18] discarding in the case of the Pearson's coefficient the staining of **4Az** at the nucleoli. On the one hand, the Pearson's coefficient is an indicator of the correlation between two images, ranging from -1 to 1 and being 1 the

indicator of a perfect correlation. On the other hand, Mander's coefficients M1 and M2 calculate the intensities of one channel co-localizing with the other. This coefficient ranges from 0 to 1 and is a good indicator even when the intensities between both channels clearly differ. Our results showed a clear correlation between MTG and **4Az** signals with a Pearson's coefficient being equal to 0.778 on average. Moreover, the Mander's coefficients also confirmed that **4Az** was located in the mitochondria. The amount of co-localization of **4Az** over MTG (M1) was 0.54 on average, whereas that of MTG over **4Az** (M2) was 0.77, which indicates that there is more MTG signal that co-localizes with **4Az** than **4Az** co-localizing with MTG. This was already expected as the **4Az** staining was also located in the cytoplasm, vesicles and nucleoli where no MTG staining is observed. Similarly, the fluorescence observed on some vesicles along the cytoplasm was predominantly associated with lysosome accumulation, as inferred from co-localization experiments with Lysotracker Green (Figure S14).

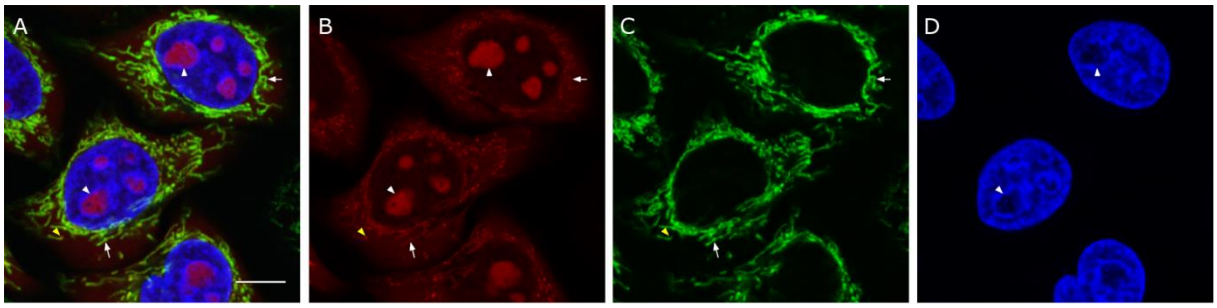

Figure 6. Co-localization studies. Single confocal plane of HeLa cells incubated with coumarin **4Az** (5 μM, red), Mitotracker Green FM (0.1 μM, green) and Hoechst 33342 (1 μg/ml, blue). A) Overlay of the three staining. B), C), D) coumarin **4Az**, Mitotracker Green FM and Hoechst 33342, separate staining, respectively. White arrows point out mitochondria, white arrowheads nucleoli and yellow arrowheads vesicles staining. Scale bar: 10 μm.

Two additional experiments were carried out to investigate accumulation of the compound inside the nucleoli. An indirect evidence of nucleoli localization was first obtained when co-staining **4Az** with Hoechst 33342 since the fluorescence emission of the coumarin dye inside the nuclei was only observed in the spots where lacked Hoechst staining (Figure 6, arrowheads). In order to further confirm the origin of the staining of nucleoli by **4Az**, we performed a ribonuclease (RNase A) digestion experiment following a previously reported procedure.[18] As shown in Figure S15, the fluorescence signal of coumarin **4Az** at the nucleoli

was completely lost after treatment with RNase, which indicates that RNA is the target of coumarin **4Az** in the nucleoli.

Overall, confocal microscopy experiments in living HeLa cells indicate that azetidinyl-COUPY fluorophores retain the cell membrane permeability of COUPY dyes, allowing visualization of specific cellular organelles, mainly mitochondria, lysosomes and nucleoli, after incubation during 30 min.

Finally, the photostability of coumarins **4Az-7Az** was also evaluated in HeLa cells by continuous irradiation with the laser beam of the confocal microscope (λ_{ex}= 561 nm for **4Az** to **6Az** and λ_{ex}= 633 nm for **7Az**). As shown in Figure 7, the overall fluorescence signal was significantly decreased in the case of coumarin **4Az**. By contrast, the intensity decrease in the case of the other fluorophores, particularly that of **6Az** and **7Az**, was minimal and mitochondria and nucleoli of HeLa cells were still clearly observed after 5 min of continuous irradiation. The higher photostability of coumarins **5Az** to **7Az**, particularly that of 4-CF_3 containing coumarins, are in good agreement with the fluorescence photobleaching results (Figure 3). Overall, azetidinyl substitution in combination with the incorporation of strong electron-withdrawing CF_3 groups at the COUPY scaffold (both at the 4-position and at the pyridyl moiety via N-alkylation) led to fluorophores with far-red/NIR emission, good cell permeability and significant high photostability.

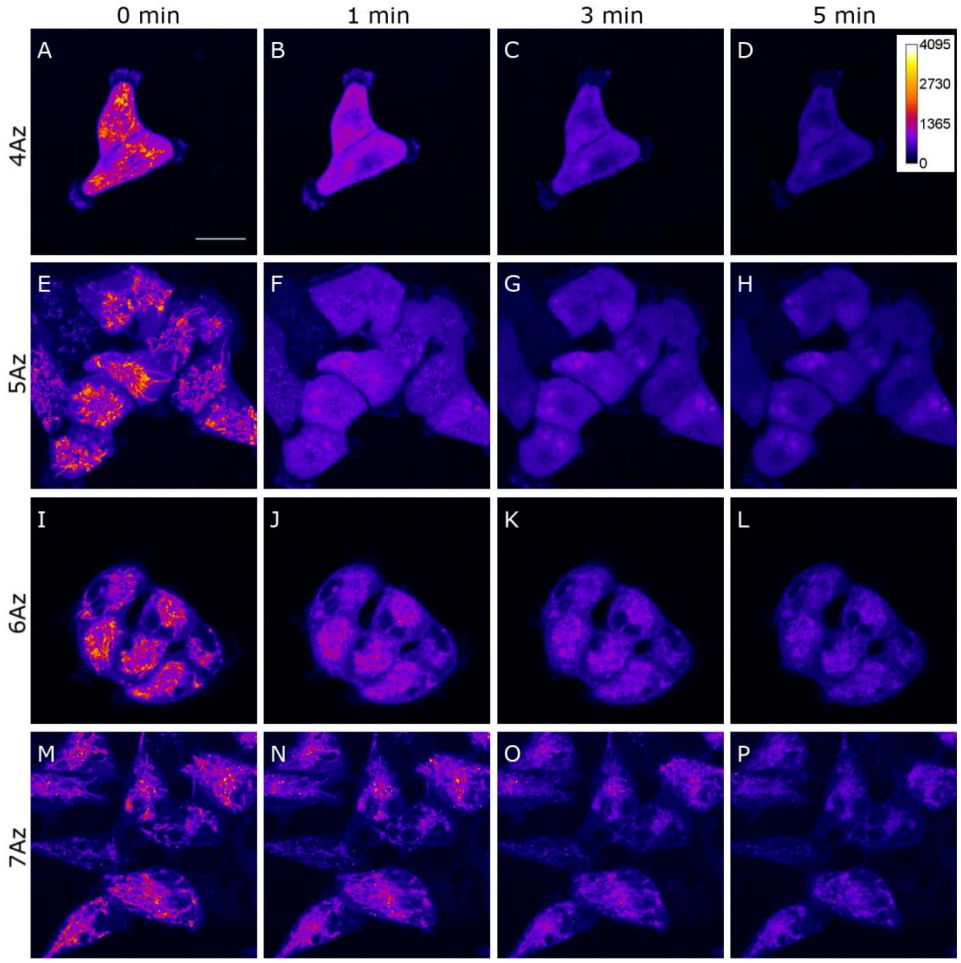

Figure 7. Photostability imaging. Single confocal planes at different time points of image acquisition are shown after incubation of HeLa cells with coumarins **4Az** to **7Az** (5 μM) during 30 min at 37 ^{o}C. Coumarins **4Az** to **6Az** were excited at 561 nm and emission detected from 570 to 670 nm, and **7Az** was excited at 633 nm and emission detected from 650 to 750 nm. Intensity calibration bar is showed in the upper right corner in D. Scale bar: 10 μm. All images are at the same scale.

CONCLUSIONS

In summary, in this work we have explored the influence of azetidinyl substitution on the photophysical and physicochemical properties of non-conventional coumarin-based COUPY dyes. First, two azetidine-containing scaffolds (**2Az** and **3Az**) were synthesized from commercially available precursors in four linear synthetic steps, the key step being the introduction of azetidinyl function at position 7 through Buchwald-Hartwig amination. The high reactivity of azetidine with Lawesson's reagent force thionation and the formation of the exocyclic C=C double bond to be performed before the incorporation of the four-membered azetidine ring. Such scaffolds were easily transformed into fluorophores **4Az**-**7Az** through *N*-alkylation of the pyridine moiety. Azetidine introduction in COUPY dyes resulted in enlarged Stokes' shifts in polar solvents with respect the *N*,*N*-dialkylamino-containing parent dyes while emission was kept in the optimal far-red/NIR region. The fluorescent quantum yield of the resulting 7-azetidinyl-COUPY fluorophores was not significantly modified in aqueous media with respect to their *N*,*N*-dialkylamino analogues, which seems to indicate that fluorescence quenching in polar media of COUPY dyes cannot be exclusively attributed to the formation of a TICT excited state or to HBIND, but to other competing de-activation channels that seem not to be efficiently arrested by azetidine. However, azetidinyl substitution led to an unprecedented improvement in photostability and high cell permeability was retained since the fluorophores accumulated selectively in mitochondria and nucleoli of HeLa cells. Overall, our results provide valuable insights for the design and optimization of novel fluorophores operating in the far-red/NIR region, since we have demonstrated that fluorescent quantum yields in polar solvents and photostability cannot be always simultaneously improved by a single structural modification such as the replacement of a *N*,*N*-dialkylamino group with azetidine, at least in non-conventional coumarin-based fluorophores like COUPY dyes.

EXPERIMENTAL SECTION

Materials and Methods

Unless otherwise stated, common chemicals and solvents (HPLC grade or reagent grade quality) were purchased from commercial sources and used without further purification. Aluminium plates coated with a 0.2 mm thick layer of silica gel 60 F_{254} were used for thin-layer chromatography analyses (TLC), whereas flash column chromatography purification was carried out using silica gel 60 (230-400 mesh). Reversed-phase high-performance liquid chromatography (HPLC) analyses were carried out on a Jupiter Proteo C_{18} column (250x4.6 mm, 90 Å 4 μm, flow rate: 1 mL/min) using linear gradients of 0.1% formic acid in H_2O (A) and 0.1% formic acid in ACN (B). NMR spectra were recorded at 25 ^oC in a 400 MHz spectrometer using the deuterated solvent as an internal deuterium lock. The residual protic signal of chloroform, methanol or DMSO was used as a reference in ^1H and ^{13}C NMR spectra recorded in $CDCl_3$, CD_3OD or DMSO-d_6, respectively. Chemical shifts are reported in part per million (ppm) in the δ scale, coupling constants in Hz and multiplicity as follows: s (singlet), d (doublet), t (triplet), q (quartet), qt (quintuplet), m (multiplet), dd (doublet of doublets), dq (doublet of quartets), br (broad signal), etc. The proton signals of the *E* and *Z* rotamers were identified by simple inspection of the ^1H spectrum and the rotamer ratio was calculated by peak integration. 2D-NOESY spectra were acquired in $CDCl_3$ or DMSO-d_6 with a mixing times of 500 ms. Electrospray ionization mass spectra (ESI-MS) were recorded on an instrument equipped with single quadrupole detector coupled to an HPLC, and high-resolution (HR) ESI-MS on a LC/MS-TOF instrument.

Synthesis of 7-azetidinyl-COUPY scaffold 2Az

*4-Methyl-7-coumarinyl-trifluoromethanesulfonate (**11a**).* The published method with some modifications was followed to synthesize compound **11a**.[15] Trifluoromethanesulfonic anhydride (1 mL, 5.9 mmol) was added dropwise to a solution of 7-hydroxy-4-methyl-coumarin **10a** (1 g, 5.7 mmol) in pyridine (30 mL) at 0 °C. After stirring for 3 h at room temperature, AcOEt (50 mL) was added to the reaction mixture, and the resulting organic phase was washed with saturated NaCl (3 × 50 mL). Then, the organic layer was successively washed with 5 % aqueous HCl (4 × 40 mL) and saturated NaCl (2 × 40 mL), dried over anhydrous Na_2SO_4 and filtered. The solvent was removed under reduced pressure to give 1.67 g (98 % yield) of a pale yellow solid which was used without further purification in the next step. TLC: R_f (DCM) 0.52; ^1H NMR (400 MHz, $CDCl_3$) δ (ppm): 7.69 (1H, d, J = 8.6 Hz), 7.28 (1H, d, J = 2.4 Hz), 7.24 (1H, dd, J = 8.6, 2.4 Hz), 6.36 (1H, br q, J = 1.2 Hz), 2.46 (3H, d, J = 1.2 Hz); $^{13}C\{^1H\}$ NMR (101 MHz, $CDCl_3$) δ (ppm): 159.6, 154.3, 151.3, 150.9, 126.5,

120.2, 118.8 (q, *J* = 322 Hz), 117.5, 116.1, 110.7, 18.9; ^{19}F NMR (376.5 MHz, $CDCl_3$): -72.6 (3F, s); LRMS (ESI-TOF) *m/z* $[M+H]^+$ calcd for $C_{11}H_8F_3O_5S^+$ 309.2, found 308.8.

*4-Methyl-2-thioxo-2H-chromen-7-yl trifluoromethanesulfonate (**12a**).* Compound **11a** (1 g, 3.2 mmol) and Lawesson's reagent (6.1 g, 15.1 mmol) were dissolved in toluene (80 mL) under an argon atmosphere. The reaction mixture was stirred at 110 °C for 4 h. After that, an additional amount of Lawesson's reagent (2 g, 4.9 mmol) was added and the reaction mixture was stirred at 110 °C overnight. The solvent was partially removed under vacuum and the mixture was filtered. After removal of the solvent under reduced pressure, the product was purified by column chromatography (silica gel, 0-8% AcOEt in hexane) to give 1.03 g (98 % yield) of a yellow solid. mp 98-99 ºC;TLC: R_f (30 % AcOEt in hexane) 0.47; ^{1}H NMR (400 MHz, $CDCl_3$) δ (ppm): 7.71 (1H, d, *J* = 8.8 Hz), 7.41 (1H, d, *J* = 2.4 Hz), 7.28 (1H, dd, *J* = 8.8, 2.4 Hz), 7.17 (1H, br q, *J* = 1.2 Hz), 2.38 (3H, d, *J* = 1.2 Hz); ^{13}C{^{1}H} NMR (101 MHz, $CDCl_3$) δ (ppm): 196.5, 156.4, 151.0, 142.3, 130.0, 126.3, 121.6, 118.8 (q, *J* = 322 Hz), 118.6, 110.4, 18.1;^{19}F NMR (376.5 MHz, $CDCl_3$): -72.5 (3F, s); HRMS (ESI-TOF) *m/z* $[M+H]^+$ calcd for $C_{11}H_8F_3O_4S_2^+$ 324.9811, found 324.9809.

*2-(Cyano(4-pyridine)methylene)-4-methyl-2H-chromen-7-yl trifluoromethanesulfonate (**13a**).* 4-Pyridylacetonitrile (317 mg, 2.68 mmol) and NaH (60 % dispersion in mineral oil, 107 mg, 2.68 mmol) were dissolved in anhydrous ACN (14 mL) under an argon atmosphere. After stirring for 30 min at room temperature, a solution of **12a** (669 mg, 2.06 mmol) in anhydrous ACN (8 mL) was added, and the reaction mixture was stirred at room temperature for 2 h and protected from light. Then, silver nitrate (456 mg, 2.68 mmol) was added and the mixture was stirred at room temperature for 90 min. The crude was evaporated under reduced pressure and purified by column chromatography (silica gel, 50-100 % DCM in hexane and 0-1.4 % MeOH in DCM). After a second purification by column chromatography (silica gel, 0-35 % AcOEt in hexane), 371 mg (44 % yield) of a yellow solid were obtained. mp 165-167 ºC; TLC: R_f (50 % AcOEt in hexane) 0.35; ^{1}H NMR (400 MHz, $CDCl_3$) δ (ppm): 8.67 (1H, dd, *J* = 4.8, 1.6 Hz), 7.70 (1H, dd, *J* = 4.8, 1.6 Hz), 7.58 (1H, m), 7.23 (1H, m), 7.21 (1H, m), 7.08 (1H, br q, *J* = 1.2 Hz), 2.42 (3H, d, *J* = 1.2 Hz); ^{13}C{^{1}H} NMR (101 MHz, $CDCl_3$) δ (ppm): 160.6, 152.5, 150.6, 150.3, 140.8, 139.2, 126.1, 121.6, 121.5, 119.2, 118.8 (q, *J* = 322 Hz), 118.2, 118.1, 110.1, 87.0, 18.7; ^{19}F NMR (376.5 MHz, $CDCl_3$): -72.56 (3F, s); HRMS (ESI-TOF) *m/z* $[M+H]^+$ calcd for $C_{18}H_{12}F_3N_2O_4S^+$ 409.0464, found 409.0467.

*7-(1-Azetidinyl)-2-(cyano(4-pyridine)methylene)-4-methyl-coumarin (**2Az**).* Azetidine (96 μL, 1.42 mmol) was added to a solution of **13a** (194 mg, 475 μmol), RuPhos-G3-palladacycle (63 mg, 71 μmol), RuPhos (35 mg, 71 μmol) and potassium carbonate (276 mg, 1.99 mmol) in

anhydrous THF (15 mL) under an argon atmosphere. The mixture was stirred at 70 °C overnight, and then the solvent was evaporated under reduced pressure. The crude was first purified by column chromatography (silica gel, 50-90 % AcOEt in hexane, dry load with Celite) and then with a HLB cartridge (C18, 10-80 % ACN in H_2O, additive: 0.1 % formic acid). After combining and freeze-drying the pure fractions, 90 mg (60 % yield) of an orange solid were obtained. mp 164-166 ºC (decomposition temperature);TLC: R_f (5 % MeOH in AcOEt) 0.44; ^{1}H NMR (400 MHz, $CDCl_3$) δ (ppm): (major rotamer) 8.58 (2H, d, *J* = 6.2 Hz), 7.75 (2H, d, *J* = 6.2 Hz), 7.33 (1H, d, *J* = 8.4 Hz), 6.77 (1H, br q, *J* = 0.8 Hz), 6.30 (1H, dd, *J* = 8.4, 2.0 Hz), 6.20 (1H, d, *J* = 2.0 Hz), 4.04 (4H, t, *J* = 7.2 Hz), 2.47 (2H, qt, *J* = 7.2 Hz), 2.34 (3H, d, *J* = 0.8 Hz); ^{13}C{^{1}H} NMR (101 MHz, $CDCl_3$) δ (ppm): (major rotamer) 163.4, 154.0, 153.9, 149.7, 144.3, 141.2, 125.4, 120.9, 119.8, 112.9, 111.2, 108.4, 96.5, 81.9, 51.9, 18.7, 16.6; HRMS (ESI-TOF) *m/z* $[M+H]^+$ calcd for $C_{20}H_{18}N_3O^+$ 316.1444, found 316.1436.

Synthesis of 7-azetidinyl-COUPY scaffold 3Az

*4-Trifluoromethyl-7-coumarinyl-trifluoromethanesulfonate (**11b**).* The published method with some modifications was followed to synthesize compound **10b**.[15] Trifluoromethanesulfonic anhydride (1.7 mL, 7.7 mmol) was added dropwise to a solution of 7-hydroxy-4-trifluoromethyl-coumarin (1.62 g, 7.0 mmol) in pyridine at 0 °C. After stirring for 5 h at room temperature, AcOEt (50 mL) was added to the reaction mixture, and the resulting organic phase was washed with saturated NaCl (3 × 50 mL). The organic layer was washed with 5 % aqueous HCl (5 × 40 mL) and saturated NaCl (2 × 40 mL), dried over anhydrous Na_2SO_4 and filtered. The solvent was removed under reduced pressure to give 2.41 g (95 % yield) of a white solid, which was used without further purification in the next step. TLC: R_f (50 % DCM in hexane) 0.46; ^{1}H NMR (400 MHz, $CDCl_3$) δ (ppm): 7.85 (1H, dq, *J* = 9.0, 1.6 Hz), 7.38 (1H, d, *J* = 2.4 Hz), 7.32 (1H, dd, *J* = 9.0, 2.4 Hz), 6.88 (1H, s); ^{13}C{^{1}H} NMR (101 MHz, $CDCl_3$) δ (ppm): 157.6, 155.1, 151.7, 140.7 (q, *J* = 33.7 Hz), 127.5 (q, *J* = 2.5 Hz), 121.3 (q, *J* = 276 Hz), 118.8 (q, *J* = 322 Hz), 118.5, 117.2 (q, *J* = 5.8 Hz), 113.7, 111.4; ^{19}F NMR (376.5 MHz, $CDCl_3$): -64.9 (3F, br s), -72.5 (3F, s); LRMS (ESI-TOF) *m/z* $[M+H]^+$ calcd for $C_{11}H_5F_6O_5S^+$ 363.2, found 362.7.

*4-Trifluoromethyl-2-thioxo-2H-chromen-7-yl trifluoromethanesulfonate (**12b**).* Compound **11b** (1.21 g, 3.3 mmol) and Lawesson's reagent (6.75 g, 16.7 mmol) were dissolved in toluene (140 mL) under an argon atmosphere. The reaction mixture was stirred for 15 h at 110 °C. The solvent was partially removed under vacuum and the mixture was filtered. After removal of the solvent under reduced pressure, the product was purified by column chromatography (silica gel, 0-16 % DCM in hexane) to give 616 mg (48 % yield) of a bright

orange solid. TLC: R_f (30 % DCM in hexane) 0.53; ^{1}H NMR (400 MHz, $CDCl_3$) δ (ppm): 7.83 (1H, dq, *J* = 8.8, 1.6 Hz), 7.46 (1H, d, *J* = 2.4 Hz), 7.45 (1H, s), 7.31 (1H, dd, *J* = 8.8, 2.4 Hz); ^{13}C{^{1}H} NMR (101 MHz, $CDCl_3$) δ (ppm): 193.7, 157.3, 151.6, 130.2 (q, *J* = 33.5 Hz), 128.7 (q, *J* = 5.9 Hz), 127.1 (q, *J* = 2.4 Hz), 122.0 (q, *J* = 276 Hz), 119.2, 118.8 (q, *J* = 322 Hz), 115.4, 110.9; ^{19}F NMR (376.5 MHz, $CDCl_3$): -64.2 (3F, br s), -72.4 (3F, s); HRMS (ESI-TOF) *m/z* $[M+H]^+$ calcd for $C_{11}H_5F_6O_4S_2^+$ 378.9528, found 378.9533.

*2-(Cyano(4-pyridine)methylene)-4-trifluoromethyl-2H-chromen-7-yl trifluoromethanesulfonate (**13b**).* 4-Pyridylacetonitrile (377 mg, 3.19 mmol) and NaH (60 % dispersion in mineral oil, 132 mg, 3.31 mmol) were dissolved in anhydrous ACN (40 mL) under an Ar atmosphere. After stirring for 30 min at room temperature, a solution **12b** (0.9 g, 2.38 mmol) in anhydrous ACN was added and the reaction mixture was stirred at room temperature for 2 h and in the dark. Then, silver nitrate (718 mg, 4.23 mmol) was added and the mixture was stirred at room temperature for 2 h. The crude was evaporated under reduced pressure and purified by column chromatography (silica gel, 0-100 % AcOEt in hexane and 0-1.5 % MeOH in AcOEt) to give to 632 mg (57 % yield) of a brown solid. mp 132-134 ºC; TLC: R_f (5 % MeOH in DCM) 0.63; ^{1}H NMR (400 MHz, DMSO-d_6) δ (ppm): 8.71 (2H, m), 8.15 (1H, d, *J* = 2.4 Hz), 7.84 (2H, m), 7.77 (1H, br dq, *J* = 8.8, 1.6 Hz), 7.55 (1H, dd, *J* = 8.8, 2.4 Hz), 7.40 (1H, s); ^{13}C{^{1}H} NMR (101 MHz, DMSO-d_6) δ (ppm): 158.3, 152.9, 150.6, 150.4, 137.5, 128.7 (q, *J* = 32 Hz), 126.4, 121.5, 121.4 (q, *J* = 275 Hz), 121.0 (q, *J* = 6 Hz), 118.8, 118.2 (q, *J* = 322 Hz), 116.9, 114.8, 111.8, 91.6; ^{19}F NMR (376.5 MHz, $CDCl_3$): -64.7 (3F, br s), -72.5 (3F, s); HRMS (ESI-TOF) *m/z* $[M+H]^+$ calcd for $C_{18}H_9F_6N_2O_4S^+$ 463.0182, found 463.0180.

*7-(1-Azetidinyl)-2-(cyano(4-pyridine)methylene)-4-trifluoromethyl-coumarin (**3Az**).* Compound **13b** (504 mg, 1.09 mmol), RuPhos-G3-palladacycle (54.1 mg, 64.7 µmol), RuPhos (29.9 mg, 64.2 µmol) and potassium carbonate (633 mg, 4.57 mmol) were dissolved in anhydrous THF (50 mL) under an argon atmosphere. Azetidine (221 µL, 3.28 mmol) was added and the mixture was stirred in the dark at 70 °C for 6 h. After removing the solvent under reduced pressure, the crude was first purified by column chromatography (silica gel, 80-100 % DCM in hexane and 0-2 % MeOH in DCM, dry load with Celite) and then with a HLB cartridge (C18, 10-80 % ACN in H_2O). After combining and freeze-drying the pure fractions, 193 mg (48 % yield) of a red solid were obtained. mp 170-172 ºC (decomposition temperature);TLC: R_f (5 % MeOH in DCM) 0.44; ^{1}H NMR (400 MHz, $CDCl_3$) δ (ppm): 8.77 (2H, d, *J* = 6.2 Hz), 8.14 (2H, d, *J* = 6.2 Hz), 7.51 (1H, br dq, *J* = 9.2, 2.0 Hz), 7.22 (1H, s), 6.40 (1H, dd, *J* = 9.2, 2.4 Hz), 6.25 (1H, d, *J* = 2.4 Hz), 4.16 (4H, t, *J* = 7.4 Hz), 2.56 (2H, qt,

J = 7.4 Hz); $^{13}C\{^{1}H\}$ NMR (101 MHz, $CDCl_3$) δ (ppm): 163.8, 155.0, 154.1, 147.2, 142.6, 136.1 (q, *J* = 33 Hz), 126.6, 122.1, 121.7 (q, *J* = 277 Hz), 116.9, 110.5 (q, *J* = 6 Hz), 109.9, 104.4, 95.6, 85.7, 51.6, 16.3; ^{19}F NMR (376.5 MHz, $CDCl_3$): (the trifluoroacetate salt of the compound was used for recording ^{19}F NMR spectrum) -63.8 (3F, d, *J* = 1.5 Hz), -75.7 (3F, s); HRMS (ESI-TOF) *m/z* $[M+H]^+$ calcd for $C_{20}H_{15}F_3N_3O^+$ 370.1162, found 370.1161.

Synthesis of 7-azetidinyl-COUPY dyes 4Az-7Az

*4-((7-(Azetidin-1-yl)-4-methyl-2H-chromen-2-ylidene)(cyano)methyl)-1-methylpyridin-1-ium trifluoromethanesulfonate (**4Az**).* Methyl trifluoromethanesulfonate (28 μL, 0.24 mmol) was added to a solution of compound **2Az** (38 mg, 0.12 mmol) in DCM (20 mL) under an Ar atmosphere. The mixture was stirred overnight at room temperature and protected from light. After removing the solvent under reduced pressure, purification by column chromatography (silica gel, 0-8.5 % MeOH in DCM) afforded 27 mg (47 % yield) of a red solid. TLC: R_f (10 % MeOH in DCM) 0.15; ^{1}H NMR (400 MHz, CD_3OD) δ (ppm): 8.45 (2H, d, *J* = 7.2 Hz), 8.19 (2H, d, *J* = 7.2 Hz), 7.71 (1H, d, *J* = 8.8 Hz), 6.96 (1H, br s), 6.64 (1H, d, *J* = 2.4 Hz), 6.60 (1H, dd, *J* = 8.8, 2.4 Hz), 4.20 (3H, s), 4.16 (4H, t, *J* = 7.4 Hz), 2.56 (3H, s), 2.52 (2H, qt, *J* = 7.4 Hz); $^{13}C\{^{1}H\}$ NMR (101 MHz, CD_3OD) δ (ppm): 168.8, 156.4, 156.2, 155.5, 151.2, 144.5, 127.8, 122.0, 119.0, 112.7, 112.2, 111.8, 96.3, 79.9, 52.7, 46.7, 19.1, 17.1; ^{19}F NMR (376.5 MHz, DMSO-d_6): -77. 8 (3F, s); HRMS (ESI-TOF) *m/z* $[M]^+$ calcd for $C_{21}H_{20}N_3O^+$ 330.1601, found 330.1598; analytical HPLC (10 to 100% B over 30 min) R_t = 11.6 min.

*4-((7-(Azetidin-1-yl)-4-methyl-2H-chromen-2-ylidene)(cyano)methyl)-1-(2,2,2-trifluoroethyl)pyridin-1-ium trifluoromethanesulfonate (**5Az**).* 2,2,2-Trifluoroethyl trifluoromethanesulfonate (60 μL, 0.42 mmol) was added to a solution of compound **2Az** (44 mg, 0.14 mmol) in anhydrous ACN (25 mL) under an Ar atmosphere. The mixture was stirred at 70 °C and protected from light for 6 h. An additional amount of 2,2,2-trifluoroethyl trifluoromethanesulfonate (30 μL, 0.21 mmol) was added to the mixture, which was stirred at 70 °C in the dark for 18 h. After removal of the major part of the solvent, the triflate salt was precipitated with cold diethyl ether, centrifuged, the solvent was decanted and the remaining solid vacuum dried. Purification by column chromatography (silica gel, 0-6 % MeOH in DCM) afforded 42 mg (56 % yield) of a dark purple solid. TLC: R_f (10 % MeOH in DCM) 0.17; ^{1}H NMR (400 MHz, DMSO-d_6) δ (ppm): 8.60 (2H, d, *J* = 7.2 Hz), 8.22 (2H, d, *J* = 7.2 Hz), 7.79 (1H, d, *J* = 8.8 Hz), 7.01 (1H, br s), 6.86 (1H, d, *J* = 2.4 Hz), 6.67 (1H, dd, *J* = 8.8, 2.4 Hz), 5.59 (2H, q, *J* = 8.3 Hz), 4.13 (4H, t, *J* = 7.4 Hz), 2.59 (3H, s), 2.45 (2H, q, *J* = 7.4 Hz); $^{13}C\{^{1}H\}$ NMR (101 MHz, DMSO-d_6) δ (ppm): (the trifluoroacetate salt of the compound was used for recording ^{13}C NMR spectrum) 167.2, 157.7 (q, *J* = 32 Hz, *TFA salt*), 154.7,

150.7, 143.7, 127.1, 123.0 (q, *J* = 279 Hz), 117.0 (q, *J* = 300 Hz, *TFA salt*), 120.4, 117.9, 111.5, 111.2, 110.9, 95.4, 78.7, 56.2 (q, *J* = 33 Hz), 51.6, 18.7, 15.8; ^{19}F NMR (376.5 MHz, CD_3OD): -73.2 (3F, t, *J* = 8.3 Hz), -80.17 (3F, s); HRMS (ESI-TOF) *m/z* $[M]^+$ calcd for $C_{22}H_{19}F_3N_3O^+$ 398.1475, found 398.1470; analytical HPLC (10 to 100% B over 30 min) R_t = 13.2 min.

*4-((7-(Azetidin-1-yl)-4-trifluoromethyl-2H-chromen-2-ylidene)(cyano)methyl)-1-methylpyridin-1-ium trifluoromethanesulfonate (**6Az**).* Methyl trifluoromethanesulfonate (26 μL, 0.23 mmol) was added to a solution of compound **3Az** (42 mg, 0.11 mmol) in DCM (20 mL) under an Ar atmosphere. The mixture was stirred overnight at room temperature and protected from light. After removal of the major part of the solvent, the triflate salt was precipitated with cold diethyl ether, centrifuged, decanted and vacuum dried. Purification by column chromatography (silica gel, 0-6 % MeOH in DCM) afforded 35 mg (60 % yield) of a purple solid. TLC: R_f (10 % MeOH in DCM) 0.22; ^{1}H NMR (400 MHz, *DMSO-d$_6$*) δ (ppm): (major rotamer) 8.75 (2H, d, *J* = 7.2 Hz), 8.29 (2H, d, *J* = 7.2 Hz), 7.52 (1H, br dq, *J* = 9.2, 2.0 Hz), 7.05 (1H, s), 6.79 (1H, d, *J* = 2.4 Hz), 6.61 (1H, dd, *J* = 9.2, 2.4 Hz), 4.27 (3H, s), 4.12 (4H, t, *J* = 7.2 Hz), 2.45 (2H, qt, *J* = 7.2 Hz); ^{13}C{^{1}H} NMR (101 MHz, $CDCl_3$) δ (ppm): (major rotamer) 165.0, 155.4, 154.7, 147.4, 145.2, 135.2 (q, *J* = 32 Hz), 126.2, 123.0, 122.3 (q, *J* = 275 Hz), 121.1 (q, *J* = 323 Hz), 117.6, 111.2, 110.2 (q, *J* = 6 Hz), 104.2, 96.9, 84.7, 51.9, 47.2, 16.3; ^{19}F NMR (376.5 MHz, CD_3OD): (major rotamer) -65.2 (3F, s), -80.2 (3F, s); HRMS (ESI-TOF) *m/z* $[M]^+$ calcd for $C_{21}H_{17}F_3N_3O^+$ 384.1318, found 384.1318; analytical HPLC (10 to 100% B over 30 min) R_t = 12.9 min.

*4-((7-(Azetidin-1-yl)-4-trifluoromethyl-2H-chromen-2-ylidene)(cyano)methyl)-1-(2,2,2-trifluoroethylpyridin-1-ium trifluoromethanesulfonate (**7Az**).* 2,2,2-Trifluoroethyl trifluoromethanesulfonate (39 μL, 0.27 mmol) was added to a solution of compound **3Az** (33 mg, 0.09 mmol) in anhydrous ACN (25 mL) under an Ar atmosphere. The mixture was stirred at 70 °C and protected from light for 8 h. The evolution of the reaction was followed by HPLC-MS and additional amounts of 2,2,2-trifluoroethyl trifluoromethanesulfonate were continuosly added (up to 2 mmol) and the reaction mixture was stirred at 70 ºC during 3 days. After removal of the major part of the solvent, the triflate salt was precipitated with cold diethyl ether, centrifuged, decanted and vacuum dried. Purification by column chromatography (silica gel, 0-5.5 % MeOH in DCM) afforded 22 mg (41 % yield) of a dark blue solid. TLC: R_f (10 % MeOH in DCM) 0.31; ^{1}H NMR (400 MHz, DMSO-*d$_6$*) δ (ppm): 8.82 (2H, d, *J* = 6.8 Hz), 8.42 (2H, d, *J* = 6.8 Hz), 7.58 (1H, br dq, *J* = 8.8 Hz), 7.10 (1H, s), 6.93 (1H, br s), 6.68 (1H, dd, *J* = 8.8, 2.0 Hz), 5.71 (2H, q, *J* = 8.8 Hz), 4.16 (4H, t, *J* = 7.6

Hz), 2.55 (2H, qt, *J* = 7.6 Hz); $^{13}C\{^{1}H\}$ NMR (101 MHz, DMSO-d_6) δ (ppm): 165.9, 155.3, 154.4, 149.6, 144.9, 135.9 (q, *J* = 32 Hz), 125.9, 122.9 (q, *J* = 280 Hz), 122.6, 121.9 (q, *J* = 276 Hz), 120.7 (q, *J* = 323 Hz), 116.9, 111.5, 109.1, 104.4, 96.3, 84.1, 56.9 (q, *J* = 34 Hz), 51.6, 15.8; ^{19}F NMR (376.5 MHz, $CDCl_3$): -64.8 (3F, d, *J* = 1.6 Hz), -72.8 (3F, t, *J* = 7.9 Hz), -80.15 (3F, s); HRMS (ESI-TOF) *m/z* $[M]^+$ calcd for $C_{22}H_{16}F_6N_3O^+$ 452.1192, found 452.1194; analytical HPLC (10 to 100% B over 30 min) R_t = 14.2 min.

Photophysical characterization of 7-azetidinyl-COUPY dyes 4Az-7Az

For the photophysical measurements, all solvents used were spectroscopic grade. Absorption spectra were recorded in a Varian Cary 6000i spectrophotometer (Varian, Palo Alto, CA) at room temperature. Molar absorption coefficients (ε) were determined by direct application of the Beer-Lambert law, using solutions of **4Az-7Az** in each solvent with concentrations ranging from 10^{-6} to 10^{-5} M. Emission spectra were registered in a Fluoromax-4 spectrofluorometer (Horiba Jobin-Ybon, Edison, NJ). Fluorescence quantum yields (Φ_F) were measured by comparative method using cresyl violet in ethanol (CV; $\Phi_{F;Ref}$ = 0.54 ± 0.03) as reference.[20] Then, optically-matched solutions of **4Az-7Az** and CV were excited and the fluorescence spectra was recorded. The absorbance of sample and reference solutions was set below 0.1 at the excitation wavelength and Φ_F were calculated using the following equation (1):

$$\phi_{F;Sample} = \frac{Area_{Sample}}{Area_{Ref}} x \left(\frac{\eta_{Sample}}{\eta_{Ref}}\right)^2 x\, \phi_{F;ref} \quad (1)$$

where $Area_{Sample}$ and $Area_{Ref}$ are the integrated fluorescence for the sample and the reference and η_{Sample} and η_{Ref} are the refractive index of sample and reference solutions respectively.

Time-resolved fluorescence decays were registered with a time-correlated single photon counting system (Fluotime 200, PicoQuant GmbH, Berlin, Germany). The samples were excited at 502 nm by means of a picosecond-pulsed LED working at 10 MHz repetition rate. Fluorescence decays were acquired at the emission maxima and they were analyzed using the PicoQuant FluoFit c4.6.5 data analysis software. The counting frequency was kept always below 1%.

The dipoles moments ($\Delta\mu$) differences between the ground (μ_g) and excited states (μ_e) for **4Az-7Az** have been estimated from the Lippert-Mataga equation:[21]

$$Stokes\ shift = \bar{\nu}_a - \bar{\nu}_f = \frac{2}{hca_0{}^3} x \left(\frac{\varepsilon - 1}{2\epsilon + 1} - \frac{n^2 - 1}{2n^2 + 1}\right) x \left(\mu_e - \mu_g\right)^2$$

$$= \frac{2}{hca_0{}^3} x\, \Delta f\, x\, \Delta\mu^2 \quad (2)$$

where h is Plank's constant, c is the velocity of light, a_0 is the radius of the Onsager cavity around the fluorophore. The parameters ε and n are the solvent dielectric constant and refractive index, respectively, which are grouped in the term Δ_f. The Onsager radius was taken as half of the average distance between the push-pull moieties of the COUPYs fluorophores as described by Mukherjee *et al*.[22]

Photostability studies were performed by monitoring fluorescence bleaching of a 5 μM **4Az-7Az** aqueous solution (PBS buffer) irradiated with green LED light (524 ± 17 nm; 7.5 mW/cm^2; LED Par 64 Short V2 lamp (Showtec, Kerkrade, The Netherlands)).

Cell culture and treatments

HeLa Cells were maintained in DMEM (Dullbecco Modified Eagle Medium) containing low glucose (1 g/L) and supplemented with 10% foetal calf serum (FCS), 50U/mL penicillin-streptomycin and 2 mM *L*-glutamine. For cellular uptake experiments and posterior observation under the microscope, cells were seeded on glass bottom dishes (P35G-1.5-14-C, Mattek). 24 h after cell seeding, cells were incubated for 30 min at 37 ºC with azetidinyl-COUPY fluorophores (**4Az-7Az**, 5 μM) in supplemented DMEM. Then, cells were washed three times with DPBS (Dulbecco's Phosphate-Buffered Saline) to remove the excess of the compounds and kept in low glucose DMEM without phenol red for fluorescence imaging. Unless otherwise stated, no fixation was carried out.

For co-localization experiments with Mitotracker Green and Hoechst 33342, HeLa cells were treated with **4Az** (5 μM) and MitoTracker Green FM (0.1 μM) for 30 min at 37 ºC in non-supplemented DMEM. After removal of the medium and washing three times with DPBS, cells were incubated for 10 min at 37 ºC with Hoechst 33342 (1 μg/ml) in supplemented DMEM. Finally, cells were washed and kept in low glucose DMEM without phenol red for fluorescence imaging.

For co-localization experiments with Lysotracker Green (0.2 μM), the same procedure as for Mitotracker Green was used but without Hoechst 33342 treatment.

For digestion experiments with RNase enzyme, HeLa cells were treated with coumarin **4Az** (5 μM) for 30 min at 37 ºC in non-supplemented DMEM. After removal of the medium and two washes with DPBS, cells were fixed with 4% paraformaldehyde (Sigma) in PBS for 10 min at RT. Then, cells were permeabilized (2 x 5 min) with PBS buffer containing glycine (20 mM) and treated with 0.05% Saponin in PBS buffer containing glycine (20 mM) for 10 min at room temperature. After permeabilization, cells were washed again (2 x 5 min) with PBS buffer containing glycine (20 mM). Finally, 25 μg/mL RNase A, DNase-free (ThermoFisher)

were added and incubated at 37 ^{o}C for 90 min. After addition of Hoechst 33342 dye and incubation at 37 ^{o}C for additional 30 min, cells were washed again twice with PBS before observation under the microscope.

For photostability studies, HeLa cells were incubated with the compounds (5 μM, 30 min at 37 ºC) and kept in low glucose DMEM without phenol red for fluorescence imaging.

Fluorescence imaging

All microscopy observations were performed using a Zeiss LSM 880 confocal microscope equipped with a 405 nm laser diode, an Argon-ion laser, a 561 nm laser and a 633 nm laser. The microscope was also equipped with a full enclosure imaging chamber (XLmulti S1, Pecon) connected to a 37 ºC heater and a 5% CO_2 providing system. Cells were observed using a 63X 1.2 multi immersion objective. Coumarins **4Az** to **6Az** were excited using the 561 nm laser and detected from 570 to 670 nm. Coumarin **7Az** was excited with the 633 nm laser and detected from 650 to 750 nm. In co-localization studies, Mitotracker Green FM and Lysotracker Green were observed using the 488 nm laser line of the Argon-ion laser whereas the 405 nm laser diode was used for observing Hoechst 33342.

In photostability studies cells were continuously irradiated every 5 s with the 561 nm laser at 15.8 μW for 5 min. Laser power was measured using a photodetector (model 818-UV, Newport) connected to an optical power meter (model 840-C, Newport).

Image analysis was performed using Fiji (1.51d).[23] Unless otherwise stated, images are colorized using Fire lookup table. In photostability studies mean intensity was measured at each time point in at least 4 different areas of 5 μm^2 at each subcellular compartment (mitochondria, cytoplasm and nucleoli) and also in areas without cells to measure the background. Images were filtered with a median filter of radius 1 to reduce noise before intensity measurements.

In co-localization studies, images were processed using Fiji. First each channel was filtered using a median filter with a radius of 1 and a Gaussian filter with a radius of 2. Then background was subtracted with a rolling ball radius of 50. To measure the Manders' coefficients a threshold including all the cytoplasm and discarding the background was set. On the other hand, the Pearson's coefficient measurements were performed after manually selecting and clearing the **4Az** signal at the nucleoli. The same selection and clearing was applied on the Mitotracker channel. Both co-localization coefficients were measured using the JaCoP plugin[18] on the different stacks of images (n=4) with each stack containing 3 to 5 cells.

ASSOCIATED CONTENT

Supporting Information

HPLC traces and UV−vis absorption and emission spectra of the compounds; additional fluorescence imaging studies; 1D NMR (^{1}H, ^{13}C, and ^{19}F), MS, and selected 2D NMR spectra (PDF).

This material is available free of charge via the Internet at http://pubs.acs.org.

AUTHOR INFORMATION

Corresponding Author

*E-mail: vmarchan@ub.edu

ACKNOWLEDGEMENTS

This work was supported by funds from the Spanish *Ministerio de Economía y Competitividad* (grants CTQ2014-52658-R, CTQ2016-78454-C2-1-R and CTQ2017-84779-R). The authors acknowledge helpful assistance of Dr. Francisco Cárdenas (NMR) and Dr. Irene Fernández and Laura Ortiz (MS) from CCiTUB. A.G. was a recipient fellow of the University of Barcelona. R.B.-O. thanks the European Social Funds and the SUR del DEC de la Generalitat de Catalunya for a predoctoral fellowship (2017 FI_B2 00140).

REFERENCES

(1) (a) Lavis, L. D.; Raines, R. T. Bright Ideas for Chemical Biology. ACS Chem. Biol. 2008, 3, 142–155; (b) Lavis, L. D.; Raines, R. T. Bright Building Blocks for Chemical Biology. ACS Chem. Biol. 2014, 9, 855–866; (c) Zheng, Q.; Juette, M. F.; Jockusch, St.; Wasserman, M. R.; Zhou, Z.; Altman, R. B.; Blanchard, S. C. Ultra-stable Organic Fluorophores for Single-molecule Research. Chem. Soc. Rev. 2014, 43, 1044–1056; (d) Lavis, L. D. Chemistry is Dead. Long Live Chemistry! Biochemistry, 2017, 56, 5165–5170.

(2) (a) *Handbook of Fluorescent Probes and Research Chemicals*, Spence, M. T. Z., Ed.; Molecular Probes, Inc., Eugene, OR, 9th edition, 2002; (b) Nani, R. R.; Kelley, J. A.; Ivanic, J.; Schnermann, M. J. Reactive Species Involved in the Regioselective Photooxidation of Heptamethine Cyanines. Chem. Sci. 2015, 6, 6556–6563; (c) Freidus, L. G; Pradeep, P.; Kumar, P.; Choonara, Y. E.; Pillay, V. Alternative Fluorophores Designed for Advanced Molecular Imaging. Drug Discov. Today 2017, 23, 115–133.

(3) (a) Frangioni, J. V. In Vivo Near-Infrared Fluorescence Imaging. Curr. Opin. Chem. Biol. 2003, 7, 626–634; (b) Owens, E. A.; Henary, M.; El Fakhri, G.; Soo Choi, H. Tissue-Specific Near-Infrared Fluorescence Imaging. Acc. Chem. Res. 2016, 49, 1731−1740; (c) Guo, Z.; Park, S.; Yoon, J.; Shin, I. Recent Progress in the Development of Near-Infrared Fluorescent Probes for Bioimaging Applications. Chem. Soc. Rev. 2014, 43, 16–29; (d) Haque, A.; Faizi, M. S. H.; Rather, J. A.; Khan, M. S. Next Generation NIR Fluorophores for Tumor Imaging and Fluorescence-Guided Surgery: A Review. Bioorg. Med. Chem. 2017, 25, 2017–2034.
(4) (a) Long, L.; Li, X.; Zhang, D.; Meng, S.; Zhang, J.; Sun, X.; Zhang, C.; Zhou, L.; Wang, L. Amino-Coumarin Based Fluorescence Ratiometric Sensors for Acidic pH and their Application for Living Cells Imaging. RSC Adv. 2013, 3, 12204–12209; (b) Schill, H.; Nizamov, S.; Bottanelli, F.; Bierwagen, J.; Belov, V. N.; Hell, S. W. 4-Trifluoromethyl-Substituted Coumarins with Large Stokes Shifts: Synthesis, Bioconjugates, and Their Use in Super-Resolution Fluorescence Microscopy. Chem. Eur. J. 2013, 19, 16556−16565; (c) Nizamov, S.; Willig, K. I.; Sednev, M. V.; Belov, V.N.; Hell, S. W. Phosphorylated 3-Heteroarylcoumarins and Their Use in Fluorescence Microscopy and Nanoscopy. Chem. Eur. J. 2012, 18, 16339–16348; (d) Nizamov, S.; Sednev, M. V.; Bossi, M. L.; Hebisch, E.; Frauendorf, H.; Lehnart, S. E.; Belov, V. N.; Hell, S. W. “Reduced” Coumarin Dyes with an O-Phosphorylated 2,2-Dimethyl-4-(hydroxymethyl)-1,2,3,4-tetrahydroquinoline Fragment: Synthesis, Spectra, and STED Microscopy. Chem. Eur. J. 2016, 22, 11631−11642.
(5) Roubinet, B; Massif, C.; Moreau, M.; Boschetti, F.; Ulrich, G.; Ziessel, R.; Renard, P. Y.; Romieu, A. New 3-(Heteroaryl)-2-iminocoumarin-based Borate Complexes: Synthesis, Photophysical Properties, and Rational Functionalization for Biosensing/Biolabeling Applications. Chem. Eur. J. 2015, 21, 14589−14601.
(6) (a) Chen, J.; Liu, W.; Zhou, B.; Niu, G.; Zhang, H.; Wu, J.; Wang, Y.; Ju, W.; Wang, P. Coumarin- and Rhodamine-Fused Deep Red Fluorescent Dyes: Synthesis, Photophysical Properties, and Bioimaging in Vitro. J. Org. Chem. 2013, 78, 6121–6130; (b) Niu, G.; Liu, W.; Wu, J.; Zhou, B.; Chen, J.; Zhang, H.; Ge, J.; Wang, Y.; Xu, H.; Wang, P. Aminobenzofuran-Fused Rhodamine Dyes with Deep-Red to Near-Infrared Emission for Biological Applications. J. Org. Chem. 2015, 80, 3170–3175.
(7) (a) Fonseca, A. S. C.; Soares, A. M. S.; Goncalves, M. S. T.; Costa, S. P. G. Thionated Coumarins and Quinolones in the Light Triggered Release of a Model Amino Acid: Synthesis and Photolysis Studies. Tetrahedron 2012, 68, 7892−7900; (b) Fournier, L.; Gauron, C.; Xu, L.; Aujard, Is.; Le Saux, T.; Gagey-Eilstein, N.; Maurin, S.; Dubruille, S.; Baudin, J.-B.;

Bensimon, D.; Volovitch, M; Vriz, S.; Jullien, L. A Blue-Absorbing Photolabile Protecting Group for in Vivo Chromatically Orthogonal Photoactivation. ACS Chem. Biol. 2013, 8, 1528−1536; (c) Fournier, L.; Aujard, I.; Le Saux, T.; Maurin, S.; Beaupierre, S.; Baudin, J.-B.; Jullien, L. Coumarinylmethyl Caging Groups with Redshifted Absorption. Chem. Eur. J. 2013, 19, 17494−17507; (d) Yamazoe, S.; Liu, Q.; McQuade, L. E.; Deiters, A.; Chen, J. K. Sequential Gene Silencing Using Wavelength-Selective Caged Morpholino Oligonucleotides. Angew. Chem., Int. Ed. 2014, 53, 10114−10118; (e) Gandioso, A.; Cano, M.; Massaguer, A.; Marchán, V. A Green Light-Triggerable RGD Peptide for Photocontrolled Targeted Drug Delivery: Synthesis and Photolysis Studies. J. Org. Chem. 2016, 81, 11556−11564, (f) Gandioso, A.; Palau, M.; Nin-Hill, A.; Melnyk, I.; Rovira, C.; Nonell, S.; Velasco, D.; García-Amorós, J.; Marchán, V. Sequential Uncaging with Green Light can be Achieved by Fine-Tuning the Structure of a Dicyanocoumarin Chromophore. ChemistryOpen 2017, 6, 375−384.

(8) Gandioso, A.; Contreras, S.; Melnyk, I.; Oliva, J.; Nonell, S.; Velasco, D.; García-Amorós, J.; Marchán, V. Development of Green/Red-Absorbing Chromophores Based on a Coumarin Scaffold That Are Useful as Caging Groups. J. Org. Chem. 2017, 82, 5398−5408.

(9) Gandioso, A.; Bresolí-Obach, R.; Nin-Hill, A.; Bosch, M.; Palau, M.; Galindo, A.; Contreras, S.; Rovira, A.; Rovira, C.; Nonell, S.; Marchán, V. Redesigning the Coumarin Scaffold into Small Bright Fluorophores with Far-Red to Near-Infrared Emission and Large Stokes Shifts Useful for Cell Imaging. J. Org. Chem. 2018, 83, 1185−1195.

(10) (a) Grimm, J. B.; English, B. P.; Chen, J.; Slaughter, J. P.; Zhang, Z.; Revyakin, A.; Patel, R.; Macklin, J. J.; Normanno, D.; Singer, R. H.; Lionnet, T.; Lavis, L. D. A General Method to Improve Fluorophores for Live-Cell and Single-Molecule Microscopy. Nat. Methods 2015, 12, 244−250. (b) Grimm, J. B.; English, B. P.; Choi, H.; Muthusamy, A. K.; Mehl, B. P.; Dong, P.; Brown, T. A.; Lippincott-Schwartz, J.; Liu, Z.; Lionnet, T.; Lavis, L. D. Bright Photoactivatable Fluorophores for Single-Molecule Imaging. Nat. Methods 2016, 13, 985−988.

(11) Liu, X.; Qiao, Q.; Tian, W.; Liu, W.; Chen, J.; Lang, M. J.; Xu, Z. Aziridinyl Fluorophores Demonstrate Bright Fluorescence and Superior Photostability by Effectively Inhibiting Twisted Intramolecular Charge Transfer. J. Am. Chem. Soc. 2016, 138, 6960−6963.

(12) (a) Singha, S.; Kim, D.; Roy, B.; Sambasivan, S.; Moon, H.; Rao, A. S.; Kim, J. Y.; Joo, T.; Park, J. W.; Rhee, Y. M.; Wang, T.; Kim, K. H.; Shin, Y. H.; Jung, J.; Ahn, K. H. A Structural Remedy Toward Bright Dipolar Fluorophores in Aqueous Media. Chem. Sci. 2015,

6, 4335−4342; (b) Shaya, J.; Fointaine-Vive, F.; Michel, B. Y.; Burger, A. Rational Design of Push–Pull Fluorene Dyes: Synthesis and Structure–Photophysics Relationship. Chem. Eur. J. 2016, 22, 10627−10637; (c) Ong, M. J. O.; Srinivasan, R.; Romieu, A.; Richard, J.-A. Divergent Synthesis of Dihydroxanthene-Hemicyanine Fused Near-Infrared Fluorophores through the Late-Stage Amination of a Bifunctional Precursor. Org. Lett. 2016, 18, 5122−5125; (d) Liu, H.; Xu, X.; Shi, Z.; Liu, K.; Fang, Y. Solvatochromic Probes Displaying Unprecedented Organic Liquids Discriminating Characteristics. Anal. Chem. 2016, 88, 10167−10175; (e) Grimm, J. B.; Brown, T. A.; Tkachuk, A. N.; Lavis, L. D. General Synthetic Method for Si-Fluoresceins and Si-Rhodamines. ACS Cent. Sci. 2017, 3, 975−985; (f) Sharma, D. K.; Adams, S. T.; Liebmann, K. L.; Miller, S. C. Rapid Access to a Broad Range of 6′-Substituted Firefly Luciferin Analogues Reveals Surprising Emitters and Inhibitors. Org. Lett. 2017, 19, 5836−5839.

(13) Bassolino, G.; Nançoz, C.; Thiel, Z.; Bois, E.; Vauthey, E.; Rivera-Fuentes, P. Photolabile Coumarins with Improved Efficiency Through Azetidinyl Substitution. Chem. Sci. 2018, 9, 387−391.

(14) Dereka, B.; Vauthey, E. Direct Local Solvent Probing by Transient Infrared Spectroscopy Reveals the Mechanism of Hydrogen-Bond Induced Nonradiative Deactivation. Chem. Sci. 2017, 8, 5057−5066.

(15) Otsuka, Y.; Sasaki, A.; Teshima, T.; Yamada, K.; Yamamoto, T. Syntheses of D-Glucose Derivatives Emitting Blue Fluorescence through Pd-Catalyzed C–N Coupling. Org. Lett. 2016, 18, 1338−1341.

(16) Ruiz-Castillo, P.; Buchwald, S. L. Applications of Palladium-Catalyzed C–N Cross-Coupling Reactions. Chem. Rev. 2016, 116, 12564−12649.

(17) Wagner, M.; Weber, P.; Bruns, T.; Strauss, W. S. L.; Wittig, R.; Schneckenburger, H. Light Dose is a Limiting Factor to Maintain Cell Viability in Fluorescence Microscopy and Single Molecule Detection. Int. J. Mol. Sci. 2010, 11, 956−966.

(18) Bolte, S.; Cordelières, F. P. A Guided Tour Into Subcellular Colocalization Analysis in Light Microscopy. J. Microsc. 2006, 224, 213-232.

(19) (a) Zhou, B.; Liu, W.; Zhang, H.; Wu, J.; Liu, S.; Xu, H.; Wang, P. Imaging of Nucleolar RNA in Living Cells Using a Highly Photostable Deep-Red Fluorescent Probe. Biosens. Bioelectron. 2015, 68, 189-196; (b) Yao, Q.; Li, H.; Xian, L.; Xu, F.; Xia, J.; Fan, J.; Du, J.; Wang, J.; Peng, X. Differentiating RNA from DNA by a Molecular Fluorescent Probe Based on the “Door-Bolt” Mechanism Biomaterials. Biomaterials 2018, 177, 78-87.

(20) Magde, D.; Brannon, J. H.; Cremers, T. L.; Olmsted, J. Absolute luminescence yield of cresyl violet. A standard for the red. J. Phys. Chem. 1979, 83, 696–699.
(21) (a) Lippert, E. Spectroscopic Determination of the Dipole Moment of Aromatic Compounds in the First Excited Singlet State. Z. Elektrochem. 1957, 61, 962–975; (b) Mataga, N.; Kaifu, Y.; Koizumi, M. Solvent Effects Upon Fluorescence Spectra and the Dipole Moments of Excited Molecules. Bull. Chem. Soc. Jpn. 1956, 29, 465–470.
(22) Mukherjee, S.; Chattopdhyay, A.; Samanta, A.; Soujanya, T. Dipole Moment Change of NBD Group Upon Excitation Studied Using Solvatochromic and Quantum Chemical Approaches: Implications in Membrane Research. J. Phys. Chem. 1994, 98, 2809–2812.
(23) Schindelin, J.; Arganda-Carreras, I.; Frise, E.; Kaynig, V.; Longair, M.; Pietzsch, T.; Preibisch, S.; Rueden, C.; Saalfeld, S.; Schmid, B.; Tinevez, J. Y.; White, D. J.; Hartenstein, V.; Eliceiri, K.; Tomancak, P.; Cardona, A. Fiji: An Open-Source Platform for Biological-Image Analysis. Nat. Methods 2012, 9, 676–682